Provision of ancillary services by renewable hybrid generation in low frequency AC systems to the grid

J. Dong[1], A. Attya[2] and O. Anaya-Lara[1]
1: Institute for Energy and Environment, University of Strathclyde, Glasgow, UK
2: Department of Engineering and Technology, University of Huddersfield, Huddersfield, UK

Abstract – Wind energy high penetration levels in power systems lead to continuous power imbalance due to the intermittent nature of wind power. This paper proposes and investigates different methods to enable a hybrid generation system to provide frequency support to the grid. The hybrid generation is 100% renewable and composed of a wind farm and hydropower plant (HPP) of comparable generation capacities, and they are interconnected through a Low Frequency AC system (LFAC). The grid–tie is composed of a Voltage-Source Converter based High-Voltage, Direct Current (VSC-HVDC) junction that acts as frequency changer to maintain the grid nominal frequency. The HPP provides two types of ancillary services: wind power smoothing and frequency drops mitigation to avoid the use of thermal generation and battery energy storage. The paper offers different control methods to provide the two AS with improved coordination between the different controls in the hybrid generation system and complying with the common requirements of Grid Codes. The results obtained show that the frequency at the LFAC can tolerate mild drops to provide frequency support to the grid. The controllers' parameters have a clear impact on the frequency response at both systems. Simulation environment is MATLAB and Simulink.

Keywords– wind power, hydropower, Ancillary services, frequency stability, low frequency AC

Nomenclature

AS: Ancillary service
WF: Wind farm
WS: Wind speed, m/s
WTG: Wind turbine generator
MPT: Maximum Power Tracking
LFAC: Low Frequency Alternating Current system
VSC-HVDC: Voltage-Source Converter High Voltage Direct Current
HPP: Hydro Power Plant
PLL: Phase-Locked Loop
PMSG: Permanent magnet synchronous generator
PMU: Phasor Measurement Unit

$P_{\mathrm{W}}^{\mathrm{f}}$: Forecasted output power of wind farm, MW

P_{W} : Actual output power of wind farm, MW

P_{d} : Subtraction between $P_{\mathrm{W}}^{\mathrm{f}}$ and P_{W}, MW

P_{H} : Actual output power of hydro turbine, MWZ

$P_{\mathrm{H}}^{\mathrm{ref}}$: Output power reference of hydro generator, per unit

$P_{\mathrm{H}}^{\mathrm{ref\_init}}$: Initial active power set-point of hydro generator, per unit

$P_{\mathrm{H}}^{\mathrm{rated}}$: Rated power of hydro generator, MW

$\Delta P_{\mathrm{H}}^{\mathrm{ref}}$: Adjustment quantity of power reference of hydro generator, per unit

P_{vsc} : Actual delivered active power of VSC station, MW

P_{vsc}^{ref} : Reference of delivered active power of VSC station, per unit

$P_{vsc}^{ref\_init}$: Initial active power set-point of VSC station, per unit

P_{vsc}^{rated} : Rated power of VSC station, MW

ΔP_{vsc}^{ref} : Active power set-point of VSC station at LFAC, per unit

$\Delta P_{vsc}^{ref\_max}$: Maximum value of ΔP_{vsc}^{ref}, per unit

Ratio A: Coefficient of VSC

Ratio B: Coefficient of hydro-power plant

Ratio A:B : Combined coefficient of VSC and hydro-power plant

RoCoF: Rate of Change of Frequency

Δf_{Grid} : Frequency deviation at Grid, Hz

T_{GCCS}^{init} : Initial time point of basic control, sec

T_{GCCS}^{peak} : Time point where ΔP_{vsc}^{ref} of basic control reaches the peak, sec

$T_{Grid}^{rec\_GCCS}$: Time point where the frequency of Grid recovers, Δf_{Grid} is less than 0.3Hz in

K_p K_i and K_d : Proportional gain, integral gain and derivative gain of PID regulator of hydro governor

H : Inertia

T_w : Water starting time of hydro turbine, sec

K_f : Damping filter gain

1 Introduction

The key challenge of maintaining the power balance between generation and demand is facing the increased penetration of wind and solar energy. Mainly because the output power of wind farms (WFs) is intermittent and difficult to forecast accurately. At low levels of wind power penetration, wind power plants can be regarded as discretely located and fluctuating negative loads, which can be resolved by the frequency regulation provided by baseline thermal generation. However, the high penetration of wind energy requires more support to compensate power more frequency and larger power imbalance. The consequent influences of generation intermittency are mainly frequency drops, transmission congestions and voltage fluctuations. Frequency drops are the main risk as they can lead to the disconnection of vulnerable generators due to the action of the Rate of Change of Frequency (RoCoF) and under frequency relays and even load shedding [1] [2] [3] [4]. In addition, WFs with conventional controls (i.e. maximum power tracking: MPT), are incapable of providing frequency support compared to synchronous power plants that dominate the current power systems. To overcome the stochastic nature of wind power generation, many researchers focused on proposing new control methods for baseline generation that relied on fossil fuel and ancillary equipment [5]. On the other hand, demand side management could be a cost-effective solution to tackle this problem, but it could affect negatively the preferences of customers, which makes it subject to consumers' resistance [6] [7]. Wind power can also provide frequency support through the widely applied techniques: droop de-loading, kinetic energy extraction and over-speeding, but they waste wind energy compared to MPT, and mitigate the efficiency of wind power collection [8].

LFAC, also known as the fractional frequency transmission system is a technology that was initially designed to deliver larger power capacities across relatively longer distances. The core idea was proposed by Wang in 1990s [9, 10]. Compared to high voltage direct and alternating current technologies (HVDC and HVAC respectively), LFAC could have economic advantages, when the distance to shore is between 50 to 200 km according to some studies [11-14] [15]. It can also extend the steady state stability compared to standard AC, due to the lower

shunt susceptance. Another advantage is that the most existing operation experience and control strategies for power generation and transmission are still functional and adoptable in LFAC as the LFAC is derived from standard AC. However, further strategies on controlling frequency changers including three phase transformer containing saturating ferromagnetic coils, phase-controlled AC-AC cycloconverter and matrix AC-AC cycloconverter were presented in [16] [17] [18] [19], where stable and quick response at power flow and voltage balancing control were exploited.

Many research focused on the control and operation of LFAC, but less effort considered the integration of hybrid generation to LFAC, which is interconnected to the Grid, and its ability to provide Ancillary Services (AS) to the Grid. This paper offers a hybrid 100% renewable generation (i.e. hydro and wind) LFAC which is enabled to provide power smoothing and frequency drops mitigation to promote the potential of using hydropower to provide frequency regulation at high penetration of renewable energy. A novel topology is adopted to connect the LFAC to the Grid, where the VSC-HVDC acts as frequency changer instead of thyristor-based cycloconverters. Such isolated generation system can be attractive for nations with several hydro and wind energy resources that are remotely located from load centres in the Grid. The HPP provides AS taking place of the conventional thermal generation and the expensive battery storage fully or partially. In particular, HPPs can provide responsive highly controllable, and sustainable frequency regulation. This capability could be curtailed by the parameters of governor controls (e.g. proportional and integral gains) and the width of the applied frequency deadband, which are commonly applied to avoid frequency overshoots at the very early stage of the event. Such isolated generation system can be attractive for nations with several hydro and wind energy resources that are remotely located from load centres in the Grid (e.g. Norway and south western areas of China). The number of pole-pairs of the HPP is selected to comply with the low synchronous speed of the LFAC. The integrated models are adapted to comply with the targeted research objectives and the investigated case studies. This includes the controller parameters, and Phase-Locked Loop (PLL) constants for the applied low frequency (50/3 Hz). A novel and simplified supplementary controller is proposed to dispatch the VSC-HVDC and the HPP to accommodate/cover surplus/deficit power between the forecasted and actual wind power. In addition, two controllers are proposed to make the HPP provide frequency support to the Grid in coordination with the VSC-HVDC station. The results obtained reveal the impact of such methods on both the frequency responses of the LFAC and the Grid. The authors have developed a comprehensive test system that includes the detailed models of the power electronics of converter stations as well as the HVDC connectors in MATALB/Simulink.

This paper exploits the novel integration of a hybrid LFAC generation system that is composed of renewable power plants, i.e. hydro-power and a WF. Moreover, three novel control methods are proposed and tested to provide wind power smoothing and frequency support services by this isolated generation system without applying special controls to the WF to avoid any undesirable reduction in the WF production. In particular, the hydropower plant is responsible for providing these services in coordination with the WF production and the Grid frequency response. The key parameters of the three control methods are carefully tuned through well-defined case studies that provide comprehensive sensitivity study of each parameter, and in relation to other factors. The credibility of the obtained results is improved through the detailed test system that includes the power electronics models, wind speed variations and full models of the WF, HPP, and the Grid.

This system can act as an attractive choice to connect offshore and onshore WFs to the Grid, as it combines the benefits of HVDC transmission systems and the LFAC system that has natural inertia and is considered as a compromise between HVDC and HVAC.

The paper is composed of six sections including this introduction. Next section explains the applied methodologies of power smoothing and frequency drops mitigation. Section 3 describes the applied case studies of power smoothing and three kinds of frequency drops mitigation. Results are discussed in Section 4, and Section 5 concludes.

2 Methodology

The strong move towards offshore wind energy includes the integration of different transmission technologies like LFAC and HVDC. This paper exploits the dynamic stability of a novel energy system that integrates a WF and a HPP that are interconnected through a LFAC. The HPP could be a hydro energy storage system or a conventional HPP [20]. The LFAC system is connected to the Grid through a HVDC junction using VSC power electronics interface as shown in Figure 1(a). In this paper, the dynamic study is focused on the role of such hybrid generation to provide frequency AS to the Grid: wind power smoothing and frequency drops mitigation.

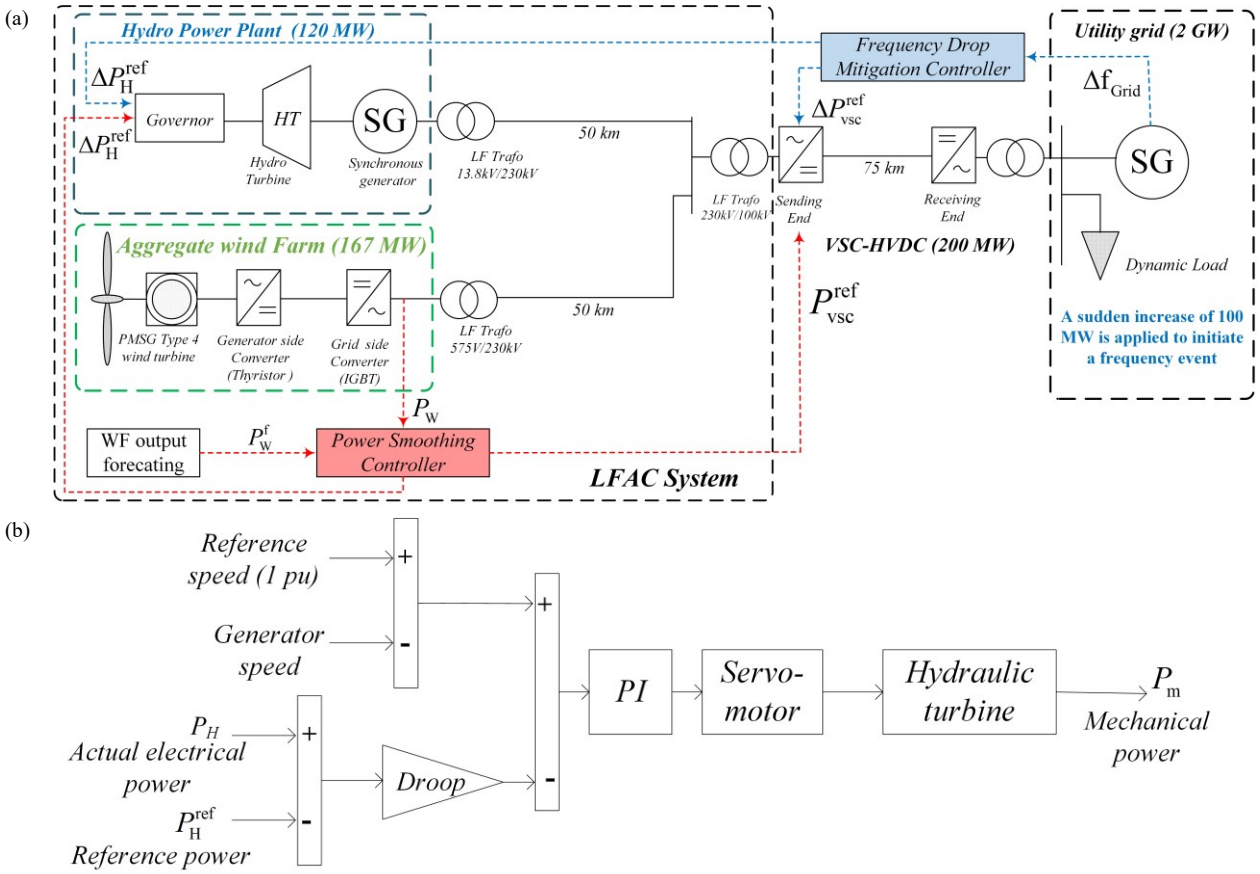

Figure 1. a) the hybrid-generation LFAC system supporting the main Grid, and b) the integrated governor

2.1 Wind power smoothing

The proposed method utilizes the HPP as a 'power buffer', which can accommodate surplus wind power and compensate insufficient wind power generation during low wind speed (WS) compared to WF output forecasts. The main references that decide whether the wind generation is below or above the generation datum is the predetermined active power set-point of the LFAC converter station (ΔP_{vsc}^{ref}), hence the power gap is evaluated using (1),

$$P_d = P_W^f - P_W \quad (P_d \text{ is proportional to } \Delta P_{vsc}^{ref}) \tag{1}$$

where P^f_w, P_w and P_d are the forecasted wind power, actual wind power and the deficit between them respectively. ΔP_{vsc}^{ref} is updated within a short time window relying on WS measurements, this could be practically applied using LIDAR technology at a certain point of the WF or separately for each wind turbine generator (WTG) [21]. The sample values of P^f_w when the WF operates at steady state under certain WSs, are recorded in Figure 2. Updating the forecast of wind generation within short-time window instead of the actual wind generation P_w allows more time for the hydro generator to react to wind generation intermittency in advance taking into consideration the relatively slower response of hydro generation. A deadband of ±0.05 pu of WF rated capacity is applied to P^f_w to curtail undesirable fluctuations as a response to very minor imbalance incidents, in addition, the rate of change of P_d is limited to 0.1 pu/s. The surplus wind power can be used to run the pumps if a hydro power energy storage is integrated. ΔP_{vsc}^{ref} is updated every 3s, while P_d is updated continuously according to the actual generation of the WF. These values are decided based on objective sensitivity studies to extend the ability to provide the required AS and improve system response. In the applied model, P_d is used to amend the reference set-point of active power provision of the HVDC sending end converter station（ΔP_{vsc}^{ref}）and the HPP (ΔP_H^{ref}) to ensure that the additional power is transmitted to the Grid as illustrated in Figure 3.

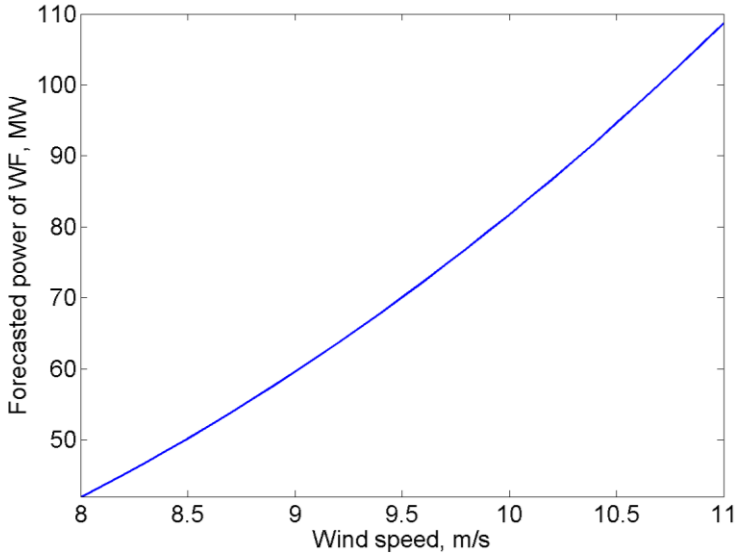

Figure 2. Forecasting of WF output for moderate wind speed

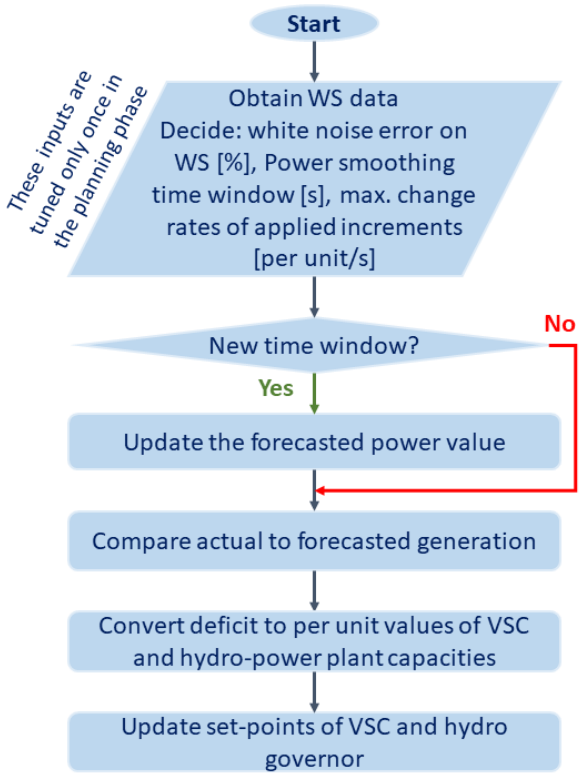

Figure 3. Power smoothing control flowchart

In the power smoothing control shown in Figure 4, P_d is updated every 3s in order to avoid very frequent changes in set-points, which can lead to large oscillations in the exported power by the VSC-station to the Grid. The proposed method converts P_d to per unit values of VSC and HPP rated power capacities, then multiplied by certain ratios using (2) and (3),

$$\Delta P_{\text{vsc}}^{\text{ref}} = Ratio\ A \frac{P_{\text{d}}}{P_{\text{vsc}}^{\text{rated}}} \tag{2}$$

$$\Delta P_{\text{H}}^{\text{ref}} = Ratio\ B \frac{P_{\text{d}}}{P_{\text{H}}^{\text{rated}}} \tag{3}$$

where Ratio A and Ratio B are the coefficients of the VSC-Sending station and HPP respectively. The purpose of these coefficients is to coordinate between the response of the HPP and the power demand of the VSC-Sending station at the LFAC. In this context, the VSC-Sending station is treated as the only load in the LFAC where the WF and HPP aim to cover this load all the times. Simultaneously, the frequency at the Grid is given the priority over the frequency at the LFAC to ensure that the users connected to the Grid are not majorly influenced by wind power fluctuations. In particular, frequency deviations could be relatively tolerated at LFAC to improve the corresponding frequency response at the Grid.

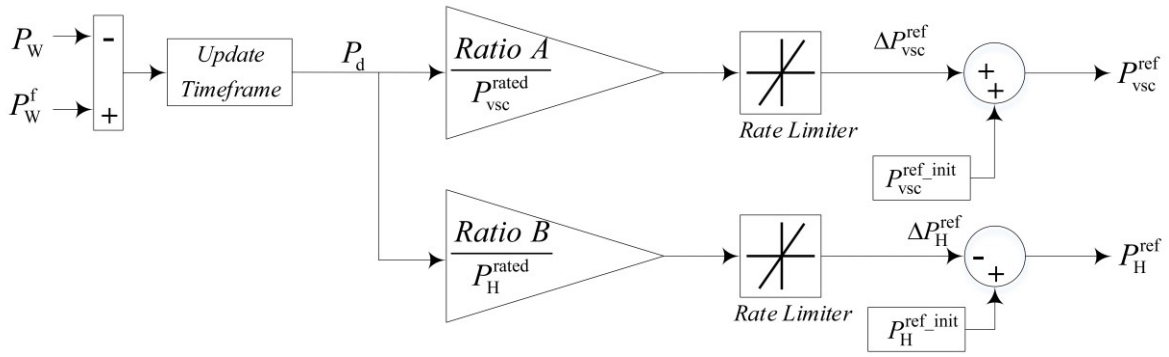

Figure 4. Model detail of power smoothing control

Finally, the reference power of VSC-Sending station (P_{vsc}^{ref}) and HPP (P_H^{ref}) are adjusted using (4) and (5), to change outputs of the VSC-Sending station and HPP to compensate P_d while the delivered active power of VSC-Sending station is smoother,

$$P_{vsc}^{ref} = P_{vsc}^{ref\_init} + \Delta P_{vsc}^{ref}$$
$$P_{vsc}^{ref} = P_{vsc}^{ref\_init} + Ratio\ A \frac{(P_W^f - P_W)}{P_{vsc}^{rated}} \quad (4)$$

$$P_H^{ref} = P_H^{ref\_init} + \Delta P_H^{ref}$$
$$P_H^{ref} = P_H^{ref\_init} + Ratio\ B \frac{(P_W^f - P_W)}{P_H^{rated}} \quad (5)$$

where P_{vsc}^{rated} and P_H^{rated} are the rated power of VSC-Sending station and HPP respectively.

2.2 Frequency drops mitigation

The proposed methods for frequency drops mitigation rely on an environment-friendly power source, which is a HPP instead of fossil fuel or battery storage to provide the required frequency support with null fuel cost. The HPP governor is able to react naturally to frequency events at the LFAC, however, the presence of the power electronics converters (i.e. the VSC station) avoids the LFAC to 'see' frequency events occurring at the Grid. Therefore, additional supplementary controllers are proposed to make the HPP respond to the events at the Grid. The communication of Grid frequency to the controls of the HPP is modelled as a time delay of 15ms for simplicity [22]. The active power set-point of the VSC station at LFAC is changed by (ΔP_{vsc}^{ref}) to provide support, and it is controlled to accommodate the additional power provided by the HPP to tackle frequency events at the Grid. The supplementary controls response to Grid events applying an immediate power step when Grid frequency violates the deadband, this imitates inertia and primary responses.

The paper proposes two methods to provide frequency support, Grid Code Compliant Support (GCCS) and an extended method that is more capable of tackling successive frequency drops (GCCS-Plus). The key measured signals used in the proposed methods are the WF output and the frequency deviation at the Grid. These two signals can be obtained by many conventional methods that are widely applied in the real-world and studied in the literature, form example Phasor Measurement Units (PMU) can be installed at the WF connection point, meanwhile PLL at the grid connection point is actually modelled in the test system, as explained in the next section, to measure the frequency of the Grid.

2.2.1 *Grid Code Compliant Support Control (GCCS)*

The relationship between the frequency deviation at the Grid (Δf_{Grid}) and ΔP_{vsc}^{ref} is depicted in Figure 5. If there is a frequency event at the Grid, the frequency support provided by the LFAC is proportional to the frequency drop at the Grid within the range between the deadband width (i.e. 50 mHz) to 0.3 Hz. The frequency events at one of the systems (i.e. LFAC and the Grid) do not have natural mutual impact on the other system due to the presence of the power electronics interface. The proposed controller allows the HPP to respond synthetically to frequency events at the Grid, providing an active power response that complies with the requirements of the Grid Code applied, which would cause frequency drops at the LFAC. However, these drops could be tolerated due to the nature of the system, and it continues for short intervals (i.e. 5s-15s). The maximum value of ΔP_{vsc}^{ref} ($\Delta P_{vsc}^{ref\_max}$) relies on the threshold of the frequency drop at LFAC that could be safely tolerated so that the VSC-Receiving station at the Grid acts provides frequency support. The occurring frequency nadir at LFAC is merely dependent on the ΔP_{vsc}^{ref}, hence $\Delta P_{vsc}^{ref\_max}$ is evaluated according to the specified acceptable frequency nadir at LFAC. A wide range of $\Delta P_{vsc}^{ref\_max}$ are examined to decide the value that does not exceed the required threshold of frequency nadir at the LFAC. The conceptual schematic of the applied supplementary control is shown in Figure 6. In this approach, the power balance will be recovered at the LFAC by the HPP, while the WF is operating normally and following MPT all the times (i.e. no frequency support by the WF). The parameters of the controller are tuned such that the provided support is comparable to the active power support of an equivalent HPP at the Grid. The controller is a proportional-integral type such that integral part is RoCoF dependant to provide synthetic inertia, while the proportional part is droop dependent. High frequency oscillations are mitigated through a low-pass filter that is represented by the transfer function shown, and the controller output is capped by $\Delta P_{vsc}^{ref\_max}$.

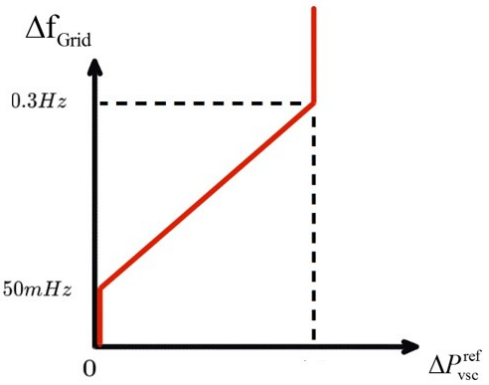

Figure 5. Relation between ΔP_{vsc}^{ref} and Δf_{Grid} at GCCS Control

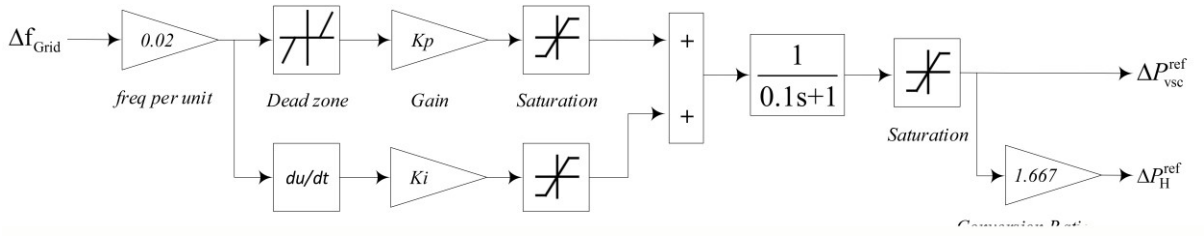

Figure 6. Schematic of the GCCS Control

2.2.2 *GCCS-Plus*

The method of GCCS-Plus has an additional merit of maintaining the power support at $\Delta P_{vsc}^{ref\_max}$ when there is a second successive frequency event at the Grid. As an illustration, when the frequency drops below the lowest threshold, the output of the HPP (i.e. $\Delta P_{vsc}^{ref\_max} + P_H^{ref}$) should be maintained *such that* P_H^{ref} *has a new value*. However, without GCCS-Plus this is not the case, as P_H^{ref} is not updated, hence when the Grid faces a second successive event the applied scheme is unable to provide any support because ΔP_{vsc}^{ref} has already reached $\Delta P_{vsc}^{ref\_max}$ as illustrated in Figure 7. The only exception for this procedure is when the HPP reaches its rated generation capacity (i.e. $P_H^{ref} \simeq 1$ pu), as there will be no room to apply further step increase in the output of the HPP. In this paper, if Δf_{Grid} is always less than 0.3 Hz during the event, this situation is considered for small frequency event as shown in Figure 7(a). The dotted blue arrow shows the tendency of ΔP_{vsc}^{ref}, which only follows the initial curve. In case of complex events with two successive frequency drops as shown in Figure 7(b), the Δf_{Grid} reaches/exceeds 0.3 Hz flagging a major frequency drop presented by the dotted blue arrow, which doesn't follow the solid normal red curve, but the dashed black border. As Δf_{Grid} recovers to the safe margin, ΔP_{vsc}^{ref} and P_H^{ref} are updated to a new value (i.e. initial $\Delta P_{vsc}^{ref\_max} + P_H^{ref}$) hence for the second event new P_H^{ref} = old $P_H^{ref} + 2\Delta P_{vsc}^{ref\_max}$ as indicated by the dotted green arrow in Figure 7(b). In summary, GCCS-Plus avoids the reduction in the delivered power by the LFAC to maintain the steady state frequency at the Grid as close to its nominal value as possible. The schematic of GCCS-Plus controller is shown in Figure 8 with the following blocks:

Basic value generator

This block realizes that when the output value of GCCS block reaches $\Delta P_{vsc}^{ref\_max}$, the output value of this block will be the sum of $\Delta P_{vsc}^{ref\_max}$ and basic value at the initial frequency event. Otherwise, the basic value will not be modified by this block.

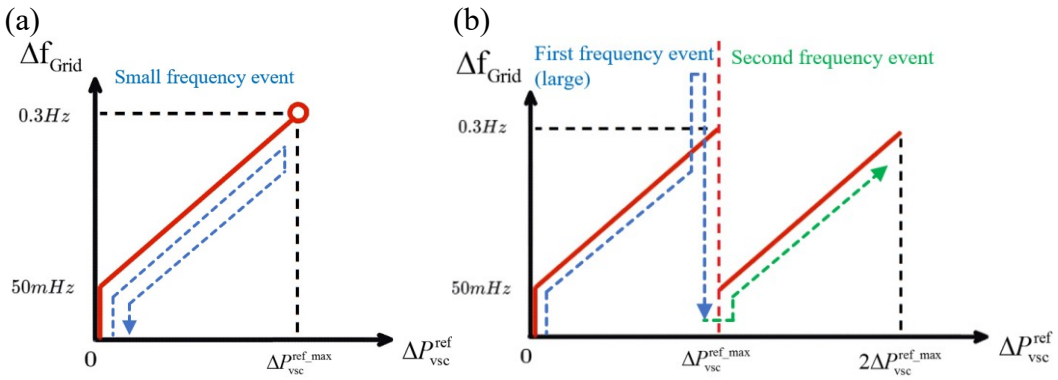

Figure 7. Relation between ΔP_{vsc}^{ref} and Δf_{Grid} in GCCS-Plus at a) minor and b) major events

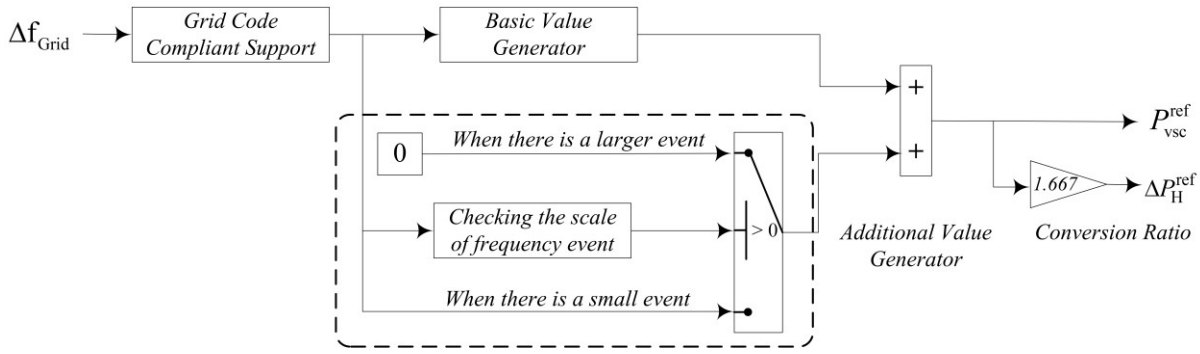

Figure 8. Schematic of GCCS-Plus

Additional value generator

This block realizes that when the output of the output of GCCS block reaches $\Delta P_{\text{vsc}}^{\text{ref\_max}}$ (i.e. there is a major frequency event at the Grid), only the first rising part of output signal of the GCCS block is transferred. It is of note that, a zero output of GCCS block is an indication that the frequency event has been declared finished. It is considered that there is a small frequency event at the Grid when the output of GCCS block (the first control method proposed in this paper) is below $\Delta P_{\text{vsc}}^{\text{ref\_max}}$.

In the context of this research, the LFAC is regarded as an isolated system, where the HPP is responsible for providing frequency support. Thus it is preferable to integrate a HPP of relatively large inertia (H) and small water starting time (T_w) to maintain a responsive power support that can contribute efficiently to frequency support at the LFAC [23]. Simultaneously, the modification of PID control of hydraulic governor is required using the set of ranges for gains of the PID controller that are given in (6).

$$\begin{aligned} 0.67\frac{H}{T_{\text{w}}} \le K_p \le 1.0\frac{H}{T_{\text{w}}} \\ 0.14\frac{H}{T_{\text{w}}^{\,2}} \le K_i \le 0.33\frac{H}{T_{\text{w}}^{\,2}} \\ 0.33H \le K_d \le 0.5H \end{aligned} \tag{6}$$

where K_p, K_i and K_d are proportional, integral and derivative gains respectively. It can be seen that the nadir of frequency of isolation mode system is dependent on the H and T_w. In addition, larger K_i and K_p are more suitable for island operation, while it is preferable to avoid derivative control (i.e. $K_d = 0$). It is worth mentioning that the parameters of an isolated HPP are different from a Grid-connected one [23]. In particular, it is necessary to ensure that the isolated system can operate steadily and improve the dynamic performance (i.e. frequency nadir and short recovery time) during the tuning of the PI controller gains of the hydropower governor. There is a certain range of typical values for K_p and K_i in the literature. For example, the work presented in [23] carried out excessive simulation tests to achieve the previously mentioned targets. The authors carried out similar approach where they applied several well designed simulation experiments to tune K_p and K_i of the hydropower governor with the new fractional synchronous frequency, and also to improve the performance when the proposed supplementary controllers are integrated. This paper is focused on primary response meanwhile further research will be dedicated to the provision of other types of AS to the Grid including secondary response.

3 Test system and case studies

The implemented test system to examine the proposed methodology is explained, followed by detailed description of the applied case studies.

3.1 Test system

The implemented test system is composed of two AC areas, a LFAC that interconnects the WF and HPP, and the other represents the Grid, where the two areas are interconnected via a low frequency link and a VSC-HVDC junction as previously shown in Figure 1. The WF is modelled as one aggregate WTG of equivalent rating of 167 MW, while the HPP has a comparable rating of 120 MW. The WTG is a Permanent Magnet Synchronous Generator (PMSG) connected via a full rated converter (i.e. Type 4 wind turbine). The system is operating at moderate wind power generation in range of 50 to 74 MW, where the initial active power set-points of the VSC-Sending station is 152.4 MW (i.e. $P_{vsc}^{ref\_init}$ = 0.762 pu), while the HPP is dispatched at 89.88 MW ($P_{H}^{ref\_init}$ = 0.749 pu). The frequency oscillations caused by power imbalance is a challenging issue for the excitation systems of the generators in LFAC, hence, it is required to re-tune the parameters of the generator exciters, for example higher damping filter gain (K_f) is applied, however this is out the scope of this paper. The technical specifications of the integrated conventional HPP governor and generator, and the power electronics converter stations and PLLs' parameters are tabulated in the appendix.

3.2 Case studies (wind power smoothing）

Two case studies are applied to exploit the wind power smoothing method. The actual and forecasted power outputs of WF are shown in Figure 9, which is applied in all the case studies and tuning procedures.

Base case: the P_{VSC} is equal to the sum of P_H and P^f_w, where P_H is the actual output power of the HPP. This case reflects the normal operation of the system.

Case 1: This case study is dedicated to check how the Ratio A influences the LFAC system and Grid, where Ratio B is set to a constant value of 0.

Case 2: The effect of Ratio B is tested in relation to the testing made in Case 1, where Ratio A is set to a constant value of 0.

The objective of these case studies is to tune Ratios A and B simultaneously to reach an optimal combination will be found out. The conventional droop control of the HPP is dedicated to tackle frequency deviations within the AC grid to which the HPP is connected. This paper adopts the conventional design of the PI droop governor of the HPP with slight changes in its proportional and integral gains. The HPP aims to provide ancillary services to the Grid, and since they are decoupled through the power electronics converters, additional controllers are proposed to enable the HPP to provide the aimed ancillary services i.e. wind power smoothing and frequency support. Actually, there is a base case where the HPP does not provide any services to the Grid, but it responds normally to the frequency deviations at the LFAC system (i.e. conventional operation).

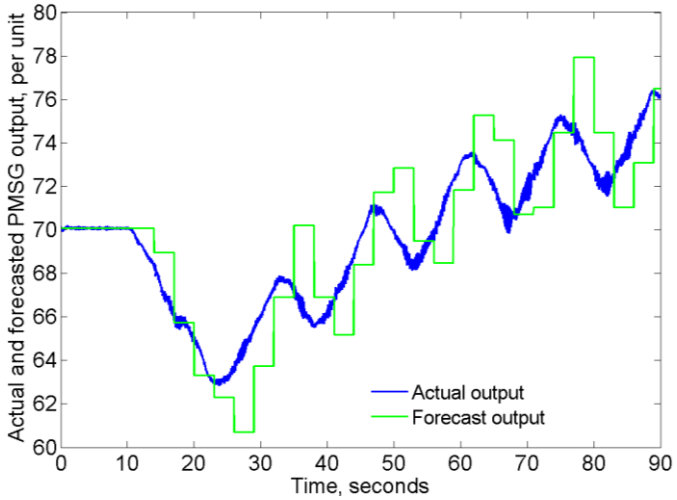

Figure 9. Simulation results: WF actual and forecasted output during the examined time interval

3.3 Case studies (frequency drops mitigation）

Two methods of frequency support for the Grid are applied to exploit the potential of frequency support provision by the HPP at the LFAC to the Grid. The Grid experiences a frequency drop triggered by a sudden load increase by 5% of the generation capacity of the Grid. There is no additional backup to support the frequency recovery at the Grid, such that the frequency support by the LFAC is investigated more clearly.

Base case: HPP is not providing frequency support to the Grid (i.e. ΔP_{vsc}^{ref} is 0 pu).

Case 1*:* Frequency support *using GCCS* where in Figure 6 $K_p = 14.29$ and $K_i = -10$.

Case 2: Frequency support *using GCCS-Plus* where in Figure 6 $K_p = 14.29$ and $K_i = -10$.

4 Results and discussion

The results obtained are highly certain due to the detailed benchmark models used to build the test system. The models of the HPP, the aggregate grid, the power electronics converters and the WF are widely used and accepted in the literature. The proposed supplementary controllers prove to have positive impact on the enhanced responses of the Grid and LFAC system compared to the base case in which the isolated system does not apply any of the proposed supplementary controls, and the isolated generation LFAC system does not provide support to the Grid. Moreover, the LFAC system is developed based on the generic per unit model of the hydro power plant in the Simulink library, where the nominal frequency and other necessary parameters are changed to obtain the equivalent system at the new fractional frequency. Following the same approach, the detailed model of the WF that is represented by an aggregate wind turbine of type 4 is obtained at the fraction frequency. The results of examining the provision of both types of AS are illustrated and discussed in the two following subsections:

4.1 Wind power smoothing

To investigate the individual influence of either Ratios, the expression Ratio A:B presents the combination of Ratio A and Ratio B respectively, where the one is set to 0 and the other is tuned to reach improved responses. Figure 10 shows the influence of Ratio A (Case 1), when it varies within the range of 0.5 to 2, the frequency deviation at Grid is mitigated gradually. However, if Ratio A exceeds 1, the wind power deficit is over-compensated (i.e. ΔP_{vsc}^{ref} is exceptionally large) leading to an intolerable deviation in the frequency deviation at LFAC. In

order to make sure that the VSC-Sending station should transfer an active power step to the Grid without severe influence on the LFAC, it is recommended that Ratio A ≤ 1.

At the beginning of wind power fluctuation, the frequency drop at LFAC is caused by wind speed deterioration as shown in Figure 11 that depicts the influence of Ratio B (Case 2). If Ratio B > 1, the frequency drop is mitigated gradually. In addition, higher values of Ratio B (e.g. Ratio B = 8) worsen the frequency nadir after the first fluctuation. It is also noticed that Ratio B does not influence the frequency at the Grid due to the presence of the VSC station. In this context, the recommended value of Ratio B is 6.

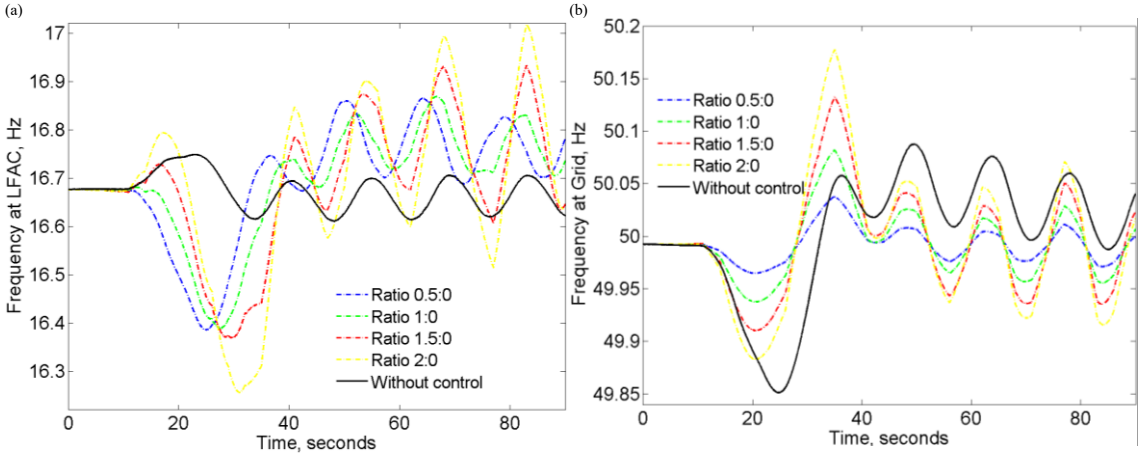

Figure 10. Simulation results: Frequency at a) LFAC and b) Grid in Case 1

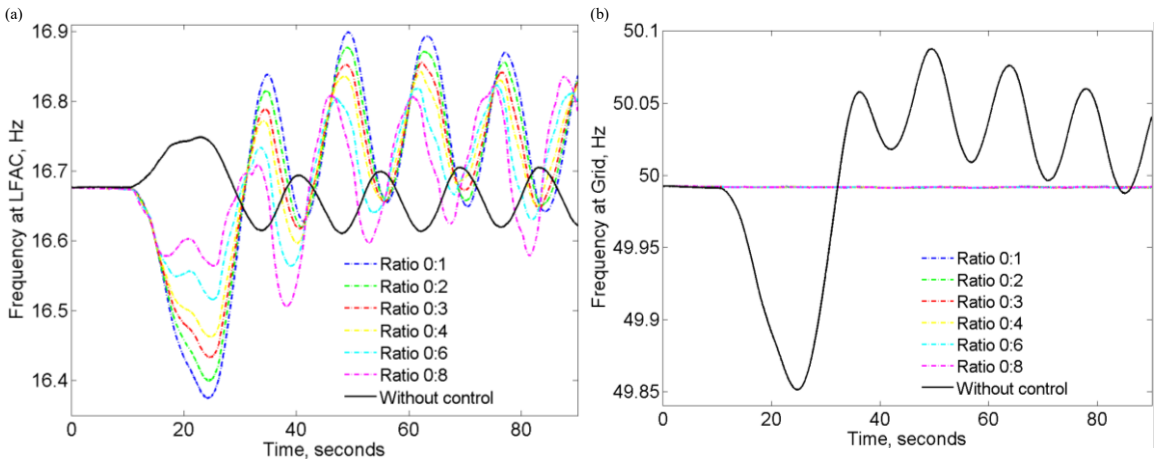

Figure 11. Simulation results: Frequency at a) LFAC and b) Grid in Case 2

After the investigation of individual influence of Ratio A and Ratio B, the preferred combination will be found by tuning Ratios A and B simultaneously. In Figure 12, it is noticed that the frequency deviation at the Grid is directly depending on the Ratio A. According to the results obtained and comparing the combinations of Ratio 0.5:0.5 to Ratio 0.5:1, the frequency deviation at LFAC can be mitigated by increasing Ratio B. Meanwhile, comparing the Ratios 0.5:0.5 and 1:0.5, the frequency deviation at LFAC can be mitigated by larger Ratio A, however, larger frequency deviation at the Grid is unfavourable consequence in that case. In this context, the preferred combination is 0.5:1. This is aligned to the outcomes of Ratio A tuning in Case 1, as Ratio < 1 improves the frequency response at the Grid.

After tuning Ratio A, it is required to tune the correspondent Ratio B. In Figure 13, the Ratio A is able to affect ΔP_{vsc}^{ref} to influence delivered power of VSC station P_{VSC} which impacts the frequency condition of Grid. Appropriate Ratio A setting can improve the P_{VSC} on power

smoothing, meanwhile the frequency deviation at LFAC is still within the tolerated margin. At the stage of tuning Ratio A, the safety margin of the Grid frequency is prioritized. The active power set-points of the generation assets at the LFAC are the key elements in tuning Ratio B. I particular, Ratio B is able to affect $\Delta P_{\mathrm{H}}^{\mathrm{ref}}$ to influence $\mathrm{P_H}$ which impacts the frequency of the LFAC. Hence, appropriate Ratio B setting results to higher frequency nadir. Ratio 0.5:4 and Ratio 0.5:6 are supposed to be the better choices through the adopted approach.

In summary, Ratio A and Ratio B are parameters that can decide how fast and intensive the VSC-Sending station and HPP respond to wind power deviations. The VSC-HVDC is based on power electronics, so $\Delta P_{\mathrm{vsc}}^{\mathrm{ref}}$ will influence $\mathrm{P_{VSC}}$ almost instantly. However, the HPP has a rotational inertia in addition to the delayed response of the servomotors controlling the gates, hence when $\Delta P_{\mathrm{H}}^{\mathrm{ref}}$ is applied, a certain time period is required to change its output power. To resolve this problem, larger Ratio B can change $\mathrm{P_H}$ in a shorter time by enlarging $\Delta P_{\mathrm{H}}^{\mathrm{ref}}$.

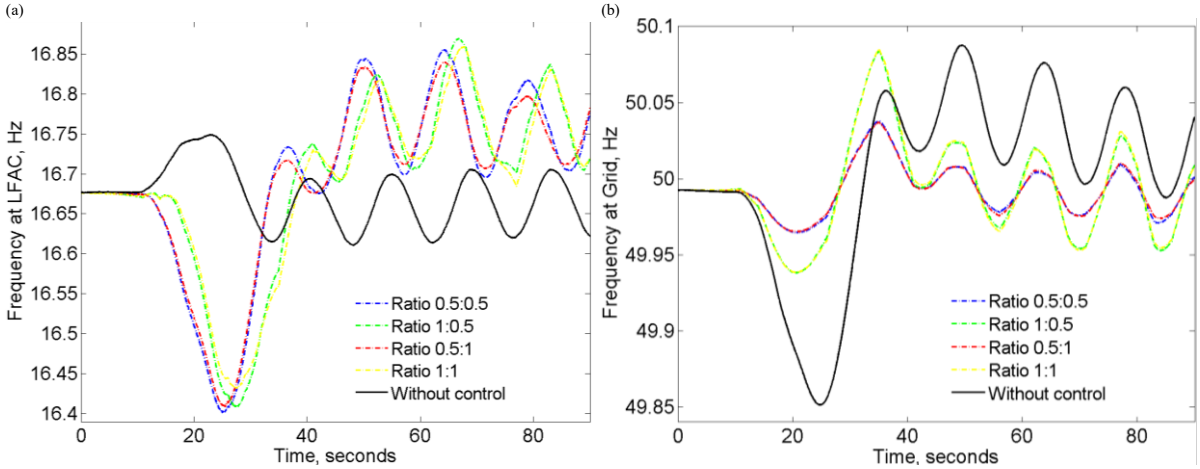

Figure 12. Simulation results: Frequency at a) LFAC and b) Grid when tuning the Ratio B

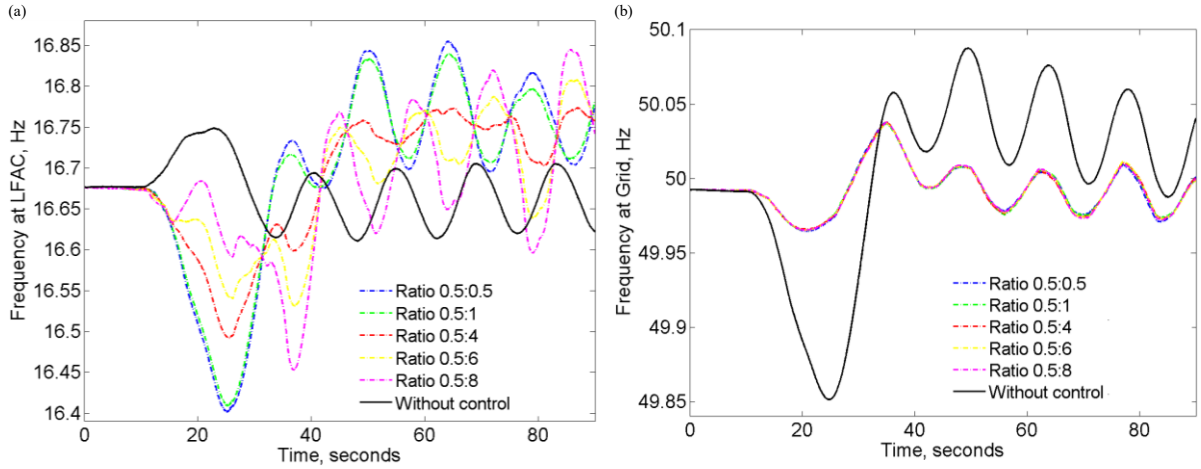

Figure 13. Simulation results: Frequency at a) LFAC and b) Grid when tuning the Ratio A

4.2 Frequency drops mitigation

In case of the GCCS, the response of the VSC-Sending station is comparable to the support provided by a conventional synchronous generator, as the frequency support is indirectly provided by the HPP at the LFAC, this is reflected in Figure 14 (a), (c) and (d). The shortage of GCCS is that there are two frequency events, a frequency nadir followed by an overshoot at LFAC as shown in Figure 14(b). In addition, the $\Delta P_{\mathrm{vsc}}^{\mathrm{ref}}$ recovers toward a zero value (i.e. $P_{\mathrm{vsc}}^{\mathrm{ref}}$ recovers towards $P_{\mathrm{vsc}}^{\mathrm{ref\_init}}$), which reduces the post-event steady state frequency at the Grid.

GCCS-Plus resolves the second event, and maintains an improved frequency deviation at the Grid. The new basic value of ΔP_{vsc}^{ref} is equal to old basic value 0.058 pu until T_{GCCS}^{peak}, where T_{GCCS}^{peak} is the time point where ΔP_{vsc}^{ref} of GCCS control reaches $\Delta P_{vsc}^{ref\_max}$, hence, the rising part in Figure 14(c) is the output value of the additional value generator shown in Figure 8. From T_{GCCS}^{init} to $T_{Grid}^{rec\_GCCS}$, the waveforms of P_{vsc}^{ref} of GCCS and GCCS-Plus are identical, where T_{GCCS}^{init} is the initial time point of GCCS control, and $T_{Grid}^{rec\_GCCS}$ is the time point where the frequency of Grid recovers above 49.7 Hz. In case of GCCS, Δf_{Grid} recovers to slightly below 0.3 Hz at $T_{Grid}^{rec\_GCCS}$, due to the curtailment in ΔP_{vsc}^{ref}. However, ΔP_{vsc}^{ref} is maintained to be at its basic value using GCCS-Plus until another frequency event starts. The impact of frequency drops mitigation methods depends on how much active power is transferred to the Grid from the LFAC. From the view point of demand side at the Grid, GCCS-Plus can offer most of the required active power instead of a conventional backup source (e.g. battery storage or thermal generation). From the view point of generation at LFAC, GCCS-Plus improves the impact on the frequency at LFAC avoiding overshoot.

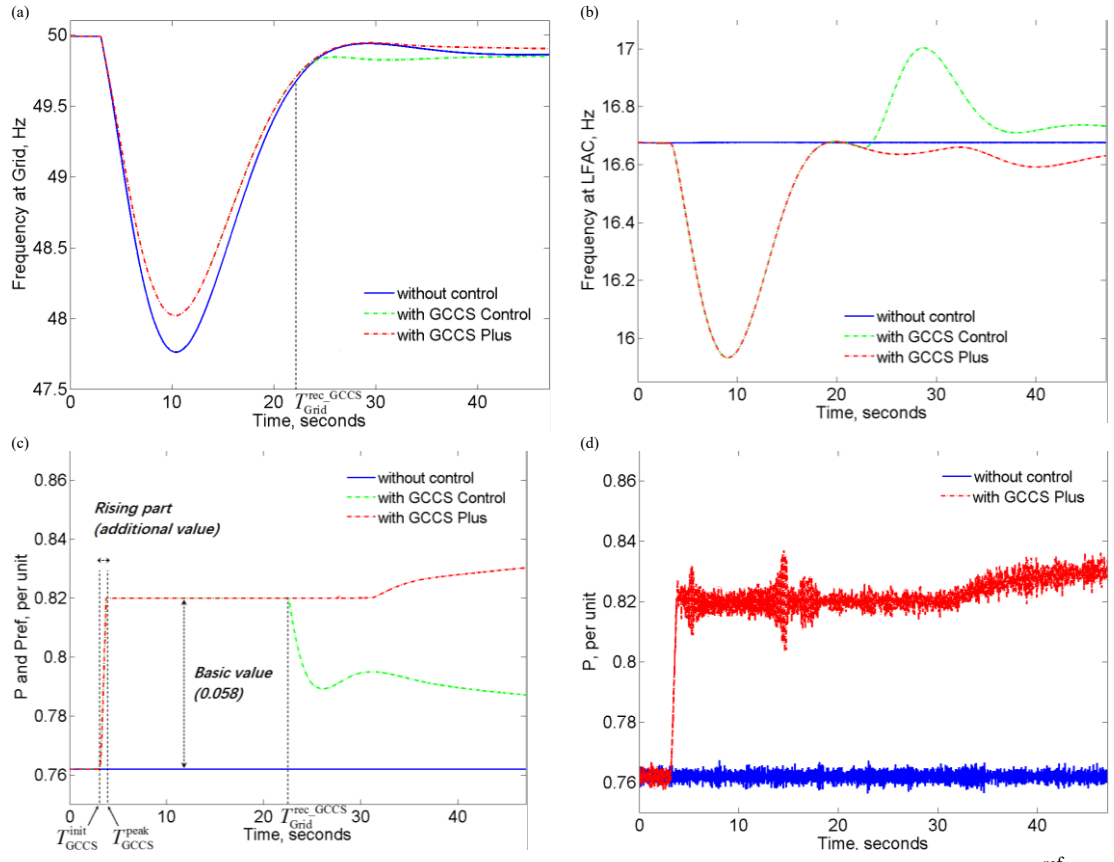

Figure 14. Simulation results: a) the Grid frequency b) the LFAC frequency c) P_{vsc}^{ref} d) P_{vsc} of control methods

5 Conclusions

This paper presents novel methods to utilise hydropower plants at LFAC power systems to offer ancillary services including power smoothing and frequency drops mitigation on behalf of wind power plants. The proposed test system that includes a hybrid 100% renewable generation system examines the ability of this island generation system to provide frequency support to the grid. Two case studies of power smoothing are analysed to find out the individual effects of two different control parameters. The best combination of these two parameters is

relative to how fast and intensive the VSC-Sending station and hydropower plant respond to the deficit between the forecasted and actual wind generation. The results obtained show improvements on the frequency response at the Grid when the parameter of the hydropower plant is tuned to much higher values compared to the parameter influencing the set-point of the VSC-Sending station.

Inertia-less generation systems like the investigated LFAC hybrid and isolated power system are enabled to provide two kinds of frequency drops mitigation control are adopted to maintain the Grid frequency within safe margins. Compared with GCCS Control, the GCCS-Plus is able to maintain the frequency at both the Grid and LFAC, meanwhile delivering more active power produced by the hydropower plant via VSC-Sending station. The Ratio A and Ratio B can be slightly higher than one to improve the provision of power smoothing, however much higher values would cause serious negative impact on the frequency stability at the LFAC. The optimal ratio combination depends on the response property of HPP and WTG. In addition, proposed frequency drops mitigation controls can improve the frequency response at the Grid including better frequency nadir and steady state frequency. In particular, the GCCS-Plus is more capable to tackle successive frequency drops and offer better frequency settling conditions for both the LFAC and the Grid. The control deviations are also investigated, for example the reference and actual power of the VSC controls. The deviations proved to be within acceptable limits and the overall positive impact of the integrated supplementary controllers to provide the aimed ancillary services is confirmed.

6 Appendix

Table 1. Hydropower plant specifications

Automatic voltage regulator and exciter		Turbine and governor	
Gain (Voltage regulator)	300	Inertia coefficient H	5s
Time constant T_a	0.001s	Proportional gain K_p	2.5
Gain K_e (Exciter)	1	Integrator gain K_i	0.25
Time constant T_e	0 s	Permanent droop R_p	0.05
Damping filter gain K_f	0.03	Water starting time T_w	2s
Time constant T_f	0.05s	Time constant T_d	0.01s

Table 2. PLLs parameters

Parameter/Network	LFAC	Grid
Frequency	16.67 Hz	50 Hz
Proportional gain K_p	2	60
Integrator gain K_i	10	1400

Table 3. Sending and Receiving end converter stations of the HVDC junction

LFAC side		Grid side	
Snubber resistance	5000 Ω	Snubber resistance	5000 Ω
Snubber capacitance	1e-6 F	Snubber capacitance	1e-6 F
Internal resistance	1e-3 Ω	Internal resistance	1e-3 Ω
DC Capacitor	2.1e-04 F	DC Capacitor	2.1e-04 F
Phase reactor (Resistance)	0.0750 Ω	Phase reactor (Resistance)	0.0750 Ω
Phase reactor (Inductance)	0.0716 H	Phase reactor (Inductance)	0.0239 H

7 References

[1] V. Ritik, K. V. Vidyanandan, and N. S. Pal, "Growing share of wind power in the power system and its impacts on frequency regulation," in *IEEE*

International Conference on Recent Trends in Electronics, Information & Communication Technology, 2017, pp. 188-194.

[2] M. H. Athari and Z. Wang, "Impacts of Wind Power Uncertainty on Grid Vulnerability to Cascading Overload Failures," *IEEE Transactions on Sustainable Energy,* vol. 9, no. 1, pp. 128-137, 2018.

[3] M. Gheydi, P. Farhadi, S. Bagheri, and A. Hematizadeh, "Impact of wind farm and thyristor-switched series capacitors in voltage, active and reactive power in normal condition of network," in *Advanced Topics in Electrical Engineering (ATEE), 2017 10th International Symposium on*, 2017, pp. 693-698: IEEE.

[4] S. Behera, M. Tripathy, and J. Satapathy, "Impacts of wind generators penetration in power systems towards voltage stability," in *Next Generation Intelligent Systems (ICNGIS), International Conference on*, 2016, pp. 1-5: IEEE.

[5] F. Díaz-González, A. Sumper, O. Gomis-Bellmunt, and R. Villafáfila-Robles, "A review of energy storage technologies for wind power applications," *Renewable and Sustainable Energy Reviews,* vol. 16, no. 4, pp. 2154-2171, 5// 2012.

[6] Z. Baharlouei and M. Hashemi, "Demand Side Management challenges in smart grid: A review," in *Smart Grid Conference (SGC), 2013*, 2013, pp. 96-101: IEEE.

[7] G. Strbac, "Demand side management: Benefits and challenges," *Energy policy,* vol. 36, no. 12, pp. 4419-4426, 2008.

[8] A. B. T. Attya and J. L. Dominguez-García, "Insights on the provision of frequency support by wind power and the impact on energy systems," *IEEE Transactions on Sustainable Energy,* 2017.

[9] W. Xifan and W. Xiuli, "Feasibility study of fractional frequency transmission system," *Power Systems, IEEE Transactions on,* vol. 11, no. 2, pp. 962-967, 1996.

[10] W. Xifan, W. Xiaohui, and M. Yongqing, "Experiment on Grid-Connection Process of Wind Turbines in Fractional Frequency Wind Power System," *Energy Conversion, IEEE Transactions on,* vol. 30, no. 1, pp. 22-31, 2015.

[11] J. Ruddy, R. Meere, and T. O'Donnell, "Low Frequency AC transmission for offshore wind power: A review," *Renewable and Sustainable Energy Reviews,* vol. 56, pp. 75-86, 4// 2016.

[12] J. Ruddy, R. Meere, and T. O'Donnell, "A Comparison of VSC-HVDC with Low Frequency AC for Offshore Wind Farm Design and Interconnection," *Energy Procedia,* vol. 80, pp. 185-192, 2015.

[13] C. N. Mau, K. Rudion, A. Orths, P. B. Eriksen, H. Abildgaard, and Z. A. Styczynski, "Grid connection of offshore wind farm based DFIG with low frequency AC transmission system," in *Power and Energy Society General Meeting, 2012 IEEE*, 2012, pp. 1-7.

[14] W. Fischer, R. Braun, and I. Erlich, "Low frequency high voltage offshore grid for transmission of renewable power," in *Innovative Smart Grid Technologies (ISGT Europe), 2012 3rd IEEE PES International Conference and Exhibition on*, 2012, pp. 1-6.
[15] X. Xiang, M. Merlin, and T. Green, "Cost analysis and comparison of HVAC, LFAC and HVDC for offshore wind power connection," 2016.
[16] W. Xi-Fan, W. Xiu-Li, and W. Jian-Hua, "Analytical approach to electric circuits containing saturating ferromagnetic coils," *Power Delivery, IEEE Transactions on,* vol. 15, no. 2, pp. 697-703, 2000.
[17] E. Gockenbach and W. Hauschild, "The selection of the frequency range for high-voltage on-site testing of extruded insulation cable systems," *Electrical Insulation Magazine, IEEE,* vol. 16, no. 6, pp. 11-16, 2000.
[18] Y. Miura, T. Mizutani, M. Ito, and T. Ise, "Modular multilevel matrix converter for low frequency AC transmission," in *Power Electronics and Drive Systems (PEDS), 2013 IEEE 10th International Conference on*, 2013, pp. 1079-1084: IEEE.
[19] R. Nakagawa, T. Funaki, and K. Matsuura, "Installation and control of cycloconverter to low frequency AC power cable transmission," in *Power Conversion Conference, 2002. PCC-Osaka 2002. Proceedings of the*, 2002, vol. 3, pp. 1417-1422: IEEE.
[20] A. B. Attya and T. Hartkopf, "Utilizing stored wind energy by hydro-pumped storage to provide frequency support at high levels of wind energy penetration," *IET Generation Transmission & Distribution,* vol. 9, no. 12, pp. 1485 - 1497, 2015.
[21] N. Wang, K. E. Johnson, and A. D. Wright, "Comparison of Strategies for Enhancing Energy Capture and Reducing Loads Using LIDAR and Feedforward Control," (in English), *IEEE Transactions on Control Systems Technology,* vol. 21, no. 4, pp. 1129-1142, 2013.
[22] K. NARENDRA and T. WEEKES, "Phasor Measurement Unit (PMU) communication experience in a utility environment," presented at the Conference on Power Systems, 2008.
[23] S. Wei, *Simulation Model of Hydraulic Turbine Regulating Systems*. Huazhong University of Science and Technology Press, 2011.